Mass Transfer Driving Forces in Packed and Fluidized Beds

GEORGE S. WILKINS and GEORGE THODOS

Northwestern University, Evanston, Illinois

The evaporation of *n*-decane into air from the surface of Celite particles, has been used for the establishment of mass transfer factors for both packed and fluidized bed systems. For these calculations log mean partial pressure differences were used. Actual concentration profiles of the transferable component were also experimentally measured by monitoring, at different bed heights, the concentration of *n*-decane vapor present in air used as the carrier gas. This was made possible through the use of an extremely sensitive hydrocarbon analyzer. The resulting profiles were used to obtain, by graphical integration, the actual driving force prevailing for each run. A nearly one-to-one correspondence was found to exist between the actual driving force and the corresponding log-mean value for both packed and fluidized bed runs.

Mass transfer studies in fluidized beds are complicated by the fact that the proper driving force associated with this transfer process is not well defined. In the past, attempts have been made to analyze mass transfer data for fluidized bed systems by assuming that the log-mean driving force applies to such a transfer process. For packed beds subjected to plug flow conditions, the application of the log-mean driving force is justified from theoretical considerations (3). However, a rigorous theoretical analysis to account for the proper driving force prevailing in a fluidized bed system is so complex as to defy a rigorous mathematical treatment. These limitations have forced earlier investigators (*1, 8*) to assume that the application of the log-mean driving force can be extended to fluidized bed systems. To obtain an answer to this ambiguous question, an experimental study was initiated specifically to establish the concentration profile of the transferable component in the carrier gas at different heights of both packed and fluidized beds.

EXPERIMENTAL EQUIPMENT

Mass transfer studies for both packed and fluidized beds involved the evaporation of *n*-decane from the surface of Celite catalyst carriers. These catalyst carriers were porous and were capable of absorbing large quantities of *n*-decane. These particles were essentially spherical and were screened to average sizes of 0.1024 and 0.1215 in. Rates of mass transfer were obtained for both packed and fluidized beds using the experimental equipment presented in Figure 1. The calming section of this experimental facility was constructed of brass and included a screen and a bed of brass spheres, ⅜ in. in diameter. This arrangement was capable of producing a uniform velocity profile of the air approaching the stainless steel porous plate (⅛ in. thick), which supported both the packed and fluidized beds.

The reactor section was constructed of Lucite tubing, I.D. = 4-7/16 in., 1/8 in. thick, and 8 in. in length. A flanged short section (3 in. in length)and a top closure constituted the rest of the unit. The top closure was made of brass and accommodated two traveling thermocouple probes and a probe for continuously withdrawing a sample of the carrier gas. Each thermocouple probe consisted of two copper-constantan thermocouples, one for measuring the temperature of the air in the fluidized bed, while the other measured the temperature of the evaporating liquid. This was accomplished by embedding a thermocouple into a single particle and cementing it in place with epoxy-resin. This particle was kept wet by soaking it with *n*-decane before each run. The length of the runs for packed and fluidized beds did not exceed the time required to approach unsteady state conditions.

A gas sample was continuously withdrawn from the axis of each packed and fluidized bed with a traveling tubular probe. The flow pattern of the fluidized bed existing under sampling conditions was visually noted to be essentially the same to that prevalent under nonsampling conditions when the sampling probe was removed from the bed. This approach enabled the continuous sampling of carrier gas over the entire bed height. This gas was monitored by continuously analyzing it for its *n*-decane content using a Beckman 109A hydrocarbon analyzer. This instrument utilized the flame ionization technique of detection and was calibrated directly for the *n*-decane content of the carrier gas leaving each bed. This was accomplished by taking advantage of the constant rate of evaporation prevalent during an experimental run. The loss in weight of the bed directly accounted for the partial pressure of *n*-decane in the effluent carrier gas. This weight loss of *n*-decane represented, for each run, the calibration point on the hydrocarbon analyzer for which a linear relationship between partial pressure and instrument reading was applied, as recommended by the manufacturer.

A run was initiated by soaking the Celite particles in *n*-decane. These wet particles were then preconditioned for approximately 2 min. by subjecting them to the flow conditions prescribed for the run. The reactor and the included preconditioned particles were rapidly weighed and were then subjected to the prescribed experimental conditions of the run. The height and pressure drop across the fluidized bed were then measured. At the termination of the run, the collapsed bed was removed and again weighed. The duration of such runs varied from 5 to 10 min. The maximum time of constant rate of evaporation was established from a preliminary trial run operating at the same mass velocity of the test run.

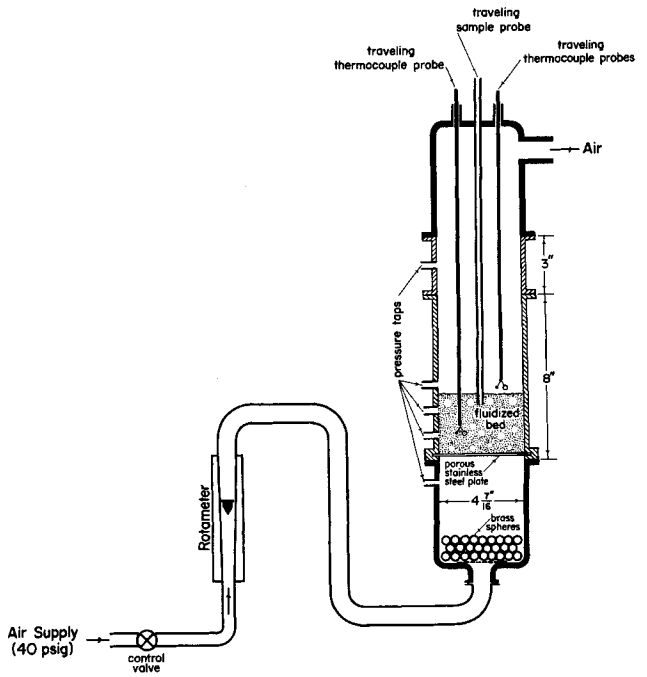

Fig. 1. Schematic diagram of experimental unit for fluidized bed studies.

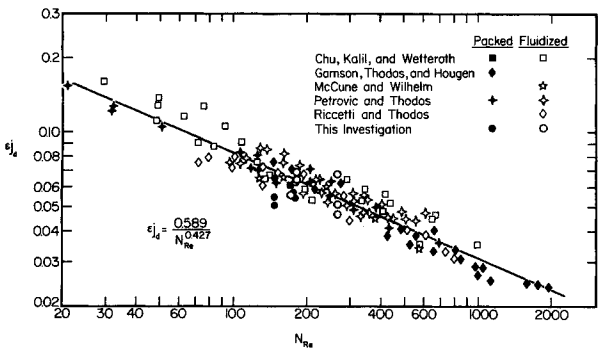

Fig. 2. Relationship between ϵj_d and N_{Re} for packed and fluidized beds resulting from the data of this study and those of others.

TREATMENT OF EXPERIMENTAL DATA

A total of thirteen runs were made by using both packed and fluidized beds. The experimental information associated with each of these runs is presented in Table 1. Of these, five were packed bed runs. For the analysis of the data of these runs, the partial pressure of the transferable component existing on the surface of the Celite particles, was calculated by using the vapor pressure relationship for *n*-decane, applicable in the temperature range of this study (9). This relationship can be expressed analytically as follows:

$$\log p = 6.71243 - \frac{1{,}218.0361}{T} - \frac{221{,}765}{T^2} \qquad (1)$$

where p is the vapor pressure in millimeters of mercury and T is the corresponding absolute temperature in °K. For room temperature conditions, the following vapor pressures of *n*-decane result from Equation (1):

°C.	°F.	p. mm.
20.0	68.0	0.949
24.0	75.2	1.27
28.0	82.4	1.67
32.0	89.6	2.19

Following a conventional approach, log-mean partial pressure differences were calculated for each packed bed run. Since the rate of evaporation of *n*-decane is relatively low, the particle surface temperature becomes essentially that of the carrier gas leaving the bed. In this regard, simultaneous mass and heat transfer calculations have been carried out for the packed bed runs. For these calculations, the simultaneous mass and heat transfer steps culminate in the relationship

$$p_s - p = \frac{h_g}{Mk_g\lambda_s}(t - t_s) \qquad (2)$$

By assuming an analogy between mass and heat transfer to apply, it can be shown that

$$p_s - p = \frac{15{,}400}{(142.3)(156)}(t - t_s) \qquad (3)$$

where λ_s = 156 B.t.u./lb., M = 142.3, and h_g/k_g = 15,400 for *n*-decane. Use of Equation (3) shows that the particle surface temperature varies slightly over the length of the bed. Furthermore, the calculated surface temperature and that obtained from the thermocouple reading at the exhaust end of the bed are in good agreement as indicated below

	Surface Temperature, °F.	
	measured	calculated
Run 15	77.0	76.8
Run 16	76.0	75.9
Run 17	74.9	74.6
Run 18	71.8	71.5
Run 19	77.0	76.8

These comparisons indicate that the temperaature difference between the measured value and the calculated surface temperature varies from 0.1 to 0.3°F. This small difference justifies the use of the outlet temperature of the carrier gas for establishing the partial pressure of *n*-decane on the surface of the particles. This method of approach was favored over the direct measurements of thermocouples embedded in particles saturated with *n*-decane.

For the packed beds, a correction for axial mixing (2) was applied to the log-mean driving force of each run, however, for the fluidized beds, such a correction is not yet justified. This correction is introduced in order to account for the existence of finger-like flow through a void. This type of flow results from the greater resistance to flow encountered near the surface of the particles surrounding a void. The driving forces of all runs, for both types of beds, are presented in Table 2. These driving forces were used to establish the mass transfer coefficient, k_g, and corresponding mass transfer factor, j_d, for each run. For these calculations, the value for the Schmidt group N_{Sc} = 3.72 calculated by Petrovic (5) was used. Values of the product ϵj_d for the packed bed runs when plotted against N_{Re}, as shown in Figure 2, are found to be in

TABLE 1. BASIC EXPERIMENTAL DATA AND CALCULATED RESULTS OF MASS TRANSFER STUDIES

Run	d_p, in.	h, in.	aV, sq. ft.	ϵ	G, lb./hr. sq. ft.	r lb./hr.	Temp., °F. t_1	Temp., °F. t_2	p_s, mm.	Δp_m, mm.	k_g lb.-moles/hr. sq. ft. atm.	j_d	ϵj_d	N_{Re}
Packed beds														
15	0.1024	1.25	4.54	0.423	768	0.632	81.4	77.0	1.35	0.575	1.41	0.126	0.0540	146
16	0.1024	1.125	4.36	0.423	770	0.644	78.0	76.0	1.30	0.514	1.71	0.153	0.0647	147
17	0.1215	1.00	3.28	0.421	765	0.545	77.7	74.9	1.24	0.654	1.48	0.133	0.0560	174
18	0.1215	1.125	3.68	0.421	770	0.480	76.5	71.8	1.10	0.540	1.29	0.126	0.0540	176
19	0.1024	1.125	4.36	0.423	765	0.636	80.8	77.0	1.35	0.647	1.30	0.112	0.0500	146
Fluidized beds														
6	0.1024	1.50	3.40	0.640	935	0.701	81.0	78.9	1.45	0.777	1.42	0.097	0.0621	178
8	0.1024	1.25	3.64	0.538	944	0.761	81.0	78.2	1.42	0.693	1.61	0.118	0.0635	180
9	0.1024	1.375	3.40	0.608	942	0.831	83.6	81.5	1.62	0.850	1.54	0.113	0.0686	179
10	0.1215	1.25	3.28	0.508	1,160	0.802	81.4	79.0	1.45	0.856	1.53	0.091	0.0462	262
11	0.1215	1.25	3.08	0.537	1,160	0.718	79.0	75.7	1.28	0.784	1.59	0.094	0.0505	263
12	0.1215	1.375	3.08	0.579	1,162	0.803	79.2	76.1	1.31	0.713	1.95	0.116	0.0671	263
13	0.1024	1.25	3.40	0.608	967	0.764	80.3	79.7	1.50	0.816	1.47	0.105	0.0636	184
14	0.1215	1.625	3.47	0.599	1,195	0.909	83.7	82.1	1.66	0.865	1.62	0.092	0.0551	170

$a(d_p = 0.1024 \text{ in.}) = 406$ sq.ft./cu.ft. $\qquad a(d_p = 0.1215 \text{ in.}) = 343$ sq.ft./cu.ft.

agreement with the results of similar studies by other investigators (*1*, *3* to *5*, *7*).

A similar treatment was used to establish the value ϵj_d for each of the fluidized bed runs. The results of calculations for Δp_m, k_g and j_d are presented in Table 1. The resulting ϵj_d values for fluidized beds were plotted against N_{Re} as shown in Figure 2 and indicate that the results of this investigation, for both packed and fluidized beds, are in agreement with the results obtained from the studies of other investigators (*1*, *3* to *5* *7*). Petrovic and Thodos (*6*) have correlated their results and those of others (*1*, *3*, *4*, *7*) to obtain for the relationship of Figure 2 the expression,

$$\epsilon j_d = \frac{0.589}{N_{Re}^{0.427}} \qquad (4)$$

The comparison between the results of the present study and those previously reported by others indicates that reasonably good agreement exists and consequently a strong inference exists that experimental information for both packed and fluidized beds can be treated similarly.

tinue to exist for approximately 0.5 in. within the bed. For bed heights beyond this distance, the partial pressure of *n*-decane in the carrier gas follows an asymptotic approach to the value of the vapor pressure prevailing on the surface of the particles.

For plug flow, the partial pressure, p, of the transferable component and bed height, z, are related by the relationship

$$p = p_s(1 - e^{\kappa z}) \qquad (5)$$

where $\kappa = k_g \pi a M_m / G$. By using the bed outlet conditions, $p = p_2$ and $z = z_2$, the constant κ was calculated for each of these runs. This approach permitted the establishment of the partial pressure profile of the transferable component indicated as dashed lines for Runs 15 and 19 shown in Figure 3. The calculated profile and that obtained from direct measurements superimpose each other for bed heights, $z \geq 0.5$ in. The deviations of partial pressures between actual and calculated values at inlet bed conditions are the result of entrance contributions which gradually diminish and disappear as the carrier gas progresses into the interior of the bed.

TABLE 2. PARTIAL PRESSURES OF *n*-DECANE IN CARRIER GAS AT DIFFERENT BED HEIGHTS OF BOTH PACKED AND FLUIDIZED BEDS

h, in.	p, mm.	h, in.	p, mm.	h, in.	p, mm.	h, in.	p, mm.	h, in.	p, mm.
Packed beds									
Run 15		Run 16		Run 17		Run 18		Run 19	
0	0	0	0	0	0	0	0	0	0
0.25	0.280	0.25	0.423	0.25	0.339	0.25	0.085	0.25	0.329
0.375	0.560	0.375	0.539	0.375	0.352	0.375	0.225	0.375	0.592
0.50	0.798	0.50	0.729	0.50	0.528	0.50	0.422	0.50	0.710
0.75	0.994	0.625	0.991	0.625	0.705	0.75	0.718	0.625	0.828
1.00	1.120	0.75	1.050	0.75	0.840	1.00	0.831	0.75	0.934
1.25	1.176	0.875	1.094	0.875	0.894	1.125	0.887	0.875	0.999
		1.00	1.137	1.00	0.949			1.00	1.065
		1.125	1.152					1.125	1.105
Fluidized beds									
Run 6		Run 8		Run 9		Run 10			
0	0	0	0	0	0	0	0		
0.25	0.359	0.25	0.247	0.25	0.442	0.25	0.284		
0.50	0.897	0.50	0.696	0.375	0.524	0.50	0.582		
0.75	1.007	0.75	0.899	0.50	0.731	0.75	0.923		
1.25	1.035	1.00	1.044	1.00	1.076	1.00	0.966		
1.50	1.076	1.25	1.157	1.25	1.159	1.25	0.997		
				1.375	1.268				
Run 11		Run 12		Run 13		Run 14			
0	0	0	0	0	0	0	0		
0.25	0.128	0.25	0.198	0.25	0.240	0.25	0.236		
0.50	0.422	0.50	0.502	0.375	0.401	0.50	0.537		
0.75	0.639	0.75	0.700	0.50	0.641	0.75	0.746		
1.00	0.767	1.00	0.884	0.75	0.855	1.00	0.838		
1.25	0.843	1.25	0.950	1.00	1.015	1.25	0.969		
		1.375	0.977	1.25	1.082	1.50	1.061		
				1.375	1.136	1.625	1.087		

AVERAGE PARTIAL PRESSURE DIFFERENCES

Packed Beds

The partial pressures of *n*-decane in the carrier gas established with the hydrocarbon analyzer at the different bed heights are summarized in Table 2. Figure 3 presents the results for Runs 15 and 19 which are typical for the packed bed runs of this study. It is interesting to note that the unusual S-shaped profiles associated with these packed bed runs do not follow throughout a logarithmic behavior postulated for plug flow through packed beds. The failure of these profiles to follow such a pattern at the inlet of the bed results from entrance effects which con-

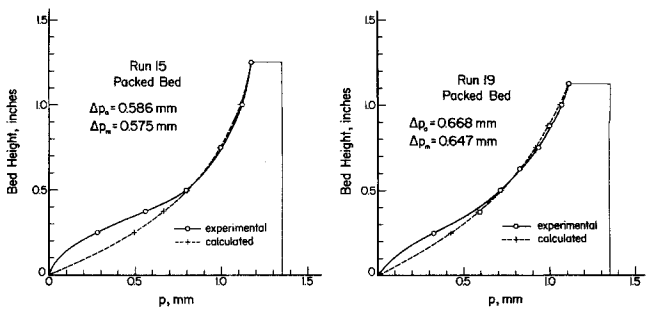

Fig. 3. Partial pressure profiles of *n*-decane in carrier gas resulting from the packed bed studies of runs 15 and 19.

Average partial pressure differences which represent the actual performance of each packed bed run were established by graphical integration. The resulting actual driving forces, Δp_a, and the corresponding log-mean driving forces, Δp_m, are summarized for the packed bed runs in Table 3. The values of Δp_a and Δp_m are nearly alike for each run and have been linked together with the relationship,

$$\Delta p_a = f \Delta p_m \qquad (6)$$

The resulting values for the packed beds were found to range from 1.019 to 1.189 for the five experimental runs. For three of these runs the values of f were 1.019, 1.032, and 1.049. For the packed bed runs f is always greater than unity. This fact can be explained from the partial pressure profiles presented in Figure 3. The actual profile of the transferable component does not follow a logarithmic behavior at the entrance of the bed and therefore the resulting values of f exceed unity.

Fluidized Beds

The n-decane partial pressure profiles for the fluidized bed runs were of a similar shape to those encountered for packed beds. Typical profiles are presented in Figure 4 for Runs 8 and 13. Actual partial pressure differences obtained by graphical integration, and corresponding calculated log-mean values are also presented in Table 3 for the fluidized bed runs. The resulting values of f for these beds ranged from 0.830 to 1.053. Five of the eight fluidized bed runs produced values of f that ranged from 0.968 to 1.028.

The results obtained from the fluidized bed data indicate that the log-mean partial pressure difference of the transferable component is nearly identical to that resulting from direct measurements. This conclusion is substantially established from the results presented in Table 3 for nearly all of the fluidized bed runs.

Table 3. Actual and Log-Mean Partial Pressure Differences of n-Decane Vapor for the Packed and Fluidized Bed Runs

Run	Δp_a, mm.	Δp_m, mm.	f
Packed beds			
15	0.586	0.575	1.019
16	0.539	0.514	1.049
17	0.726	0.654	1.110
18	0.642	0.540	1.189
19	0.668	0.647	1.032
Fluidized beds			
6	0.645	0.777	0.830
8	0.730	0.693	1.053
9	0.823	0.850	0.968
10	0.796	0.856	0.930
11	0.806	0.784	1.028
12	0.718	0.713	1.007
13	0.810	0.816	0.993
14	0.844	0.865	0.976

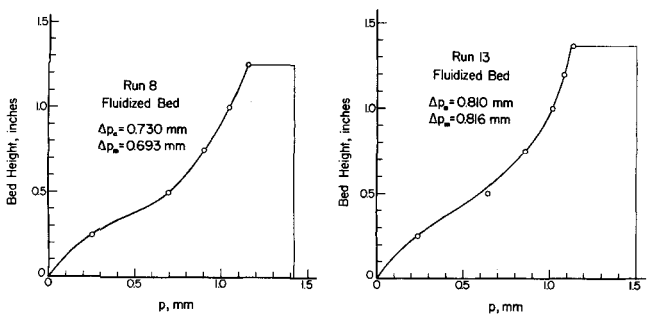

Fig. 4. Partial pressure profiles of n-decane in carrier gas resulting from the fluidized bed studies of runs 8 and 13.

ACKNOWLEDGMENT

The authors are grateful to the Phillips Petroleum Company for supplying the n-decane used is this study.

NOTATION

a = total interfacial area of packing, sq.ft./cu.ft.
d_p = particle diameter, in.
D_p = particle diameter, ft.
D_v = diffusivity of binary system, sq.ft./hr.
f = factor, Equation (4)
G = superficial mass velocity, lb./hr.sq.ft.
h = bed height, in.
h_g = heat transfer coefficient, B.t.u./hr.sq.ft. °F.
j_d = mass transfer factor, $(k_g p_{gf} M_m/G)(\mu/\rho D_v)_f^{2/3}$
k_g = mass transfer coefficient, lb.-moles/hr.sq.ft. atm., $r/aV\Delta p_m$
M = mean molecular weight of carrier gas
N_{Re} = particle Reynolds number, $D_p G/\mu$
p = partial pressure of transferable component, mm. Hg.
p_{gf} = partial pressure of nontransferable component, atm.
p_s = vapor pressure of transferable component on surface of particle, mm. Hg.
Δp_a = driving force obtained by graphical integration, mm. Hg.
Δp_m = log-mean driving force, mm. or atm.
r = rate of mass transfer, lb./hr.
N_{Sc} = Schmidt group, $\mu/\rho D_v$
t = temperature, °F.
t_s = temperature of particle surface, °F.
T = absolute temperature, °K.
V = volume of bed, cu.ft.
z = bed height, ft.

Greek Letters

ϵ = void fraction
κ = constant, Equation (5)
λ_s = latent heat of vaporization of transferable component at temperature of particle surface, °F.
μ = absolute viscosity, lb./hr.ft.
π = total pressure, atm.
ρ = density, lb./cu.ft.

LITERATURE CITED

1. Chu, J. C., J. Kalil, and W. A. Wetteroth, *Chem. Eng., Progr.*, **49**, 141 (1953).
2. Epstein, N., *Can. J. Chem. Eng.*, **36**, 210 (1958).
3. Gamson, B. W., George Thodos, and O. A. Hougen, *Trans. Am. Inst. Chem. Eng.*, **39**, 1 (1943).
4. McCune, L. K., and R. H. Wilhelm, *Ind. Eng. Chem.*, **41**, 1124 (1949).
5. Petrovic, L. J., Ph.D. dissertation, Northwestern Univ., Evanston, Ill. (1967).
6. ———, and George Thodos, Paper presented at the *Intern. Symp. Fluidization*, Eindhoven, The Netherlands, (June, 1967).
7. Riccetti, R. E., and George Thodos, *AIChE J.*, **7**, 443 (1961).
8. Sen Gupta, Ashis, and George Thodos, *Chem. Eng. Progr.*, **58**, 58 (1962).
9. Thodos, George, unpublished data.

Manuscript received August 3, 1967; revision received July 26, 1968; paper accepted July 29, 1968.